Journal of the Brazilian Society of Mechanical Sciences and Engineering (2022) 44: 445
https://doi.org/10.1007/s40430-022-03758-7

TECHNICAL PAPER

New slip-line field model based on dead metal zone and material flow ın negative rake orthogonal cutting

Erhan Altan[1] · **Uğur Emiroğlu**[1]

Received: 20 January 2022 / Accepted: 24 August 2022 / Published online: 5 September 2022

Abstract
A new slip-line field model for orthogonal cutting with negative rake angle tools was proposed in this study. The presence of a dead metal zone in front of a cutting tool with a negative rake angle and also bidirectional material flow was considered in the new model. According to this model, a partial of the removal material becomes chip, while the rest moved downward into the workpiece. Cutting forces and the amount of the depth of cut that moved downward into the workpiece were determined by using this model. Under particular cutting conditions, orthogonal cutting experiments were carried out using a shaping-based computer-controlled quick stop device. It was experimentally observed that the material exhibited bidirectional flow during cutting with tool having negative rake angle. The amount of materials in both formations: material moved toward onto the cutting tool and under it, changed depending on the cutting conditions and the variation of negative rake angle. Additionally, the position of the stagnation point which determines the material flow was defined by the model. Finally, it was seen that the experimental and analytical results were in good agreement.

Keywords Negative rake angle · Slip-line field model · Material flow · Orthogonal cutting

Abbreviations

V	Cutting speed
γ	Rake angle
τ	Shear flow stress
β	Prow angle
φ	Shear angle
Ψ	θ Slip-line angles
W	Width of cut
t_0	Depth of cut
t_1	Position of stagnation point
t_2	Amount of material moving to the under of cutting tool
t_3	Height from A to H in the model
h	Height from E to D in the model
F_c	Cutting force
F_{cc}	Calculated cutting force from model
F_{cm}	Measured cutting force
F_t	Thrust force
F_{tc}	Calculated thrust force from model
F_{tm}	Measured thrust force
m	Friction factor
k	Material shear flow stress
P_1	Normal stress act along AC
P_2	Normal stress act along CD
P_3	Normal stress act along DE
M_1	Initial weight of the workpiece
M_2	Final weight of the workpiece
t_{2c}	Calculated t_2 from the model
t_{2m}	Obtained t_2 from the experiments
a	Height of workpiece

1 Introduction

Machining is the chip removal process that is widely used in the manufacturing industry. The cutting mechanism of the process, especially cutting with negative rake angle, has still been under investigation. Negative rake angle cutting tools provide superior tool wedge strength, longer tool life and low chipping compared to the cutting tools with positive rake angle. In particular, cutting with tool having negative rake angle is preferred for materials with poor machinability. Therefore, single point cutting tools with negative rake angle

Technical Editor: Adriano Fagali de Souza.

✉ Uğur Emiroğlu
emiroglu@yildiz.edu.tr

[1] Department of Mechanical Engineering, Yildiz Technical University, Istanbul, Turkey

are extensively employed for machining of these materials. In addition, the cutting mechanism of abrasive grains in the grinding process is similar to the cutting mechanism of the cutting tool with negative rake angle. All mentioned issues point out that more study is needed to understand cutting mechanism in case of negative rake angle cutting tools.

Researchers have conducted some studies to explain the cutting mechanism of cutting tools with negative rake angle. In these studies, changes in cutting and thrust forces, dead metal zone and material flow were studied. One of the early studies related to modeling of cutting with tool having negative rake angle, which was valid for continuous chip formation, was made by Connolly and Rubenstein [1]. Kopalinsky and Oxley [2] experimentally investigated the effect of rake angle on cutting force and thrust force by using the cutting tools having negative rake angle between 5° and − 25°. The experimental results showed that ratio of cutting forces increased with the increase in negative rake angle. Abdelmoneim and Scrutton [3] studied the changes of cutting forces in machining of zinc and brass with negative rake angle tools and reported that no chips were formed at rake angle of -80°. Abdelmoneim et al. [4] investigated the effects of rake angle, cutting speed and depth of cut on cutting and thrust forces in machining of brass with cutting tools having negative rake angle at low cutting speeds. They stated that, the chip thickness decreased as the rake angle became negative and no chips were formed higher than the rake angle of − 75,5°. Findley and Reed [5] showed that chip was formed at the rake angle of -60° in orthogonal machining. Ding et al. [6] investigated the critical negative rake angle in orthogonal machining of aluminum and copper alloys. They argued that the critical negative rake angle (− 77° for aluminum and -81° for copper alloy) had a significant effect on the surface roughness and residual stresses.

In the previous studies, different critical negative rake angle values which do not create chip have been found. However, it has not been reported that the amount of material that forms the chip, changes with the negative rake angle value of cutting tool.

In the grinding process, since the cutting mechanism of the abrasive grains has the feature of cutting tool with negative rake angle [7, 8], some researchers also worked in this area by using pyramidal, conical and spherical cutting tools with negative rake angle. Sedriks and Mulhearn [9] applied pyramidal tungsten carbide tools to solve cutting and rubbing mechanics in simulated abrasive processes. Lortz [10] developed a physical model to explain the mechanisms of friction, plowing, cutting using a spherical cutting edge tool in grinding. Kita et al. [11–13] studied the cutting mechanism by using a conical cutting tool that was likened to an abrasive grain with a large negative rake angle and they developed a quick stop technique for their experiments. The researchers suggested that a stagnant zone occurred in machining with cutting tools having negative rake angle. They also claimed that the material flow was bidirectional. Komanduri [14] proposed some approaches of machining with negative rake tools by simulating grinding. He claimed that no chips were formed at -85°, and the material flow on the tool surface was bidirectional. Ohbuchi and Obikawa [15, 16] modeled the orthogonal cutting with large negative rake angles by using finite element method for simulating grinding process with abrasive grains. They noticed that a stagnant region ahead of the tool tip acts as a stable edge in cutting tools with large negative rake angles. Doyle [17] studied the cutting mechanism in grinding with abrasive particles having large negative rake angles using the quick stop technique and he reported a discontinuous type of chip in single grit grinding at low cutting speed.

Slip-line field theory has been recognized as one of the most effective tools for modeling chip formation in metal cutting [18]. Researchers also carried out slip-line modeling studies with negative rake angle cutting tools. Abebe and Appl [19] developed the slip-line model to explain the mechanics of cutting with negative rake angle cutting tools and it was observed the dead metal zone directed the material flow. Kita et al. [20] studied the behavior of material flow in front of a negative rake tool surface by developing a new shear line model. Fang [21] expanded the physical slip-line model of Lee-Schafer [22] and developed a slip-line model for the negative rake angle cutting tools. According to Fang [21], the dead metal zone changed with the change of cutting speed. Vinogradow [23] proposed a geometric model and conducted experimental studies to understand the chip formation mechanism using a cutting tool with negative rake angle. Researcher noted that a comparison between the calculated and experimental values of chip–formation characteristics reveals a fairly good fit for the values of the tangential component of the chip–formation force. Zou and Sheethaler [24] presented a slip-line model for orthogonal cutting with chamfered tools with negative rake angle. They noted that the physical model considered the flow of the material below the cutting tool, and however, the upper part of the field in the model approximated with an existing model developed by Yellowley [25]. This model has limited usefulness when the chamfer angle is too much negative. A slip-line model was developed to examine the dead metal zone and cutting mechanism in orthogonal machining with cutting tools having negative rake angle [26, 27]. It was observed that the thrust force increased slightly up to about -40° of rake angle, and then, sharp rise has been seen up to -70°. The researchers stated that the dead metal zone widens as the negative rake angle becomes more negative. Hu et al. [28] proposed a slip-line model for dead metal zone formation for cutting temperature prediction with chamfered insert with negative rake angle. They pointed out that the comparison result indicated that the developed thermal model gave satisfactory prediction of the temperature distribution and maximum cutting temperatures. Manjunathaiah and Endres [29] developed a model of cutting with rounded edge tools that effect as a tool having negative rake angle. They developed a machining force model by conducting a force balance on the lower boundary of the deformation zone. Researchers pointed out that the increase in specific energy with edge radius is not only due to the energy dissipated in deforming the machined surface but also substantially due to the energy expended in shearing the chip, as introduced by a more negative average rake angle.

It is known that if there is a cutting edge radius in the tool tip geometry or especially when edge radius is applied to the cutting tools, a negative rake angle effect due to radius is observed in the cutting mechanism. Shiva et al. [30] studied an experimental investigation to assess the effects of trumpet hone on tool life and surface quality in milling of AISI4140 steel. They determined that trumpet honed edge was found to produce the surface with lower and constant surface roughness values compared to symmetric edge. The influence of edge preparation on coated carbide cemented tool milling of aluminum alloy was investigated by Zhao et al. [31] using DEFORM simulations and cutting experiments. Zeilman et al. [32] studied characterization of edge preparation processes and the impact on surface integrity after milling of AISI P20 steel. Padmakumar and Shiva [33] focused on the effect of form factor on forces, surface roughness, and spindle power in face milling of AISI 4140 steel.

In the previous studies, the cutting mechanism in the machining with the cutting tool having negative rake angle was investigated. In these studies, only assumptions about the material flow were made and it was stated that the material flow was bidirectional from the cutting tool surface. However, a detailed experimental study and a slip-line field model related to material flow behavior are not seen. The amount of material going under the cutting tool and its mechanism were not specified in the literature. In addition, dead zone point is important for machining, and however, there are some studies on the position of the dead zone point in the literature [26, 34, 35].

In this study, a new slip-line field model was developed for orthogonal cutting with negative rake angle cutting tool. Experiments were carried out with a cutting tool with negative rake angle under certain cutting conditions for orthogonal cutting. It was shown in the developed model that the flow of the material was bidirectional. Material in one direction of the flow formed as chip and in the other direction material moved downward into the workpiece. The amount of the depth of cut which moved downward into the workpiece was determined. Theoretical calculations were also made for determining the position of the dead metal zone. The results of experimental studies and model were compared, and the generated model was validated by using material flow and cutting forces.

2 Proposed slip-line field model

The proposed new slip-line field model for the cutting tool with negative rake angle in orthogonal chip removal is given in Fig. 1. Material flow is bidirectional in the model. The arrowed lines on the figure show the flow of workpiece material both into the chip and under the cutting tool during cutting. A part of the removed material forms chip, and the other part goes downward into the workpiece from the material separation point. The GJE zone is the dead metal zone, and the "J" is the separation point of the material flow. The material in the dead metal zone was considered as stagnant.

Some basic assumptions were made for the solution of the developed model such as considering the workpiece material as rigid and plastic. The workpiece material properties do not change with strain, strain rate and temperature. This slip-line model applies to orthogonal chip removal with continuous chip formation. It is assumed that the material flow occurs according to the stationary stagnant zone and occurs without a built-up edge.

HE is a slip-line and represents the traditional shear plane inclined at the shear angle φ. In the slip-line model, there is material accumulation in front of the cutting tool. The prow zone is defined at angle of β with respect to the uncut workpiece surface. The vertical distance between the uncut workpiece surface and the machined workpiece surface refers to the depth of cut "t_0." The material flowing to the under of the cutting tool is the "t_2," part of the depth of cut. "t_1" is the height of the stagnation point, and it is the distance from the J point to the cutting surface that determines the material flow.

The field under the HE slip-line can be determined by considering the frictional and geometric relationships. Due to the high normal stress at the dead zone and the workpiece boundary JE, a constant frictional stress τ can be considered proportional to the material shear flow stress k and can be written as;

$$\tau = m * k \tag{1}$$

where m is the friction factor, and k is the material shear flow stress.

Since very high strains, strain rates and temperatures are involved in machining, k can be determined from orthogonal cutting experiments [36].

$$k = \frac{Fc.\cos\phi - Ft.\sin\phi}{w * \frac{HE}{1000}} \tag{2}$$

where F_c is the cutting force, F_t is the thrust force, φ is the shear angle, and w is the cutting width.

The angles of Ψ and θ are expressed as follows;

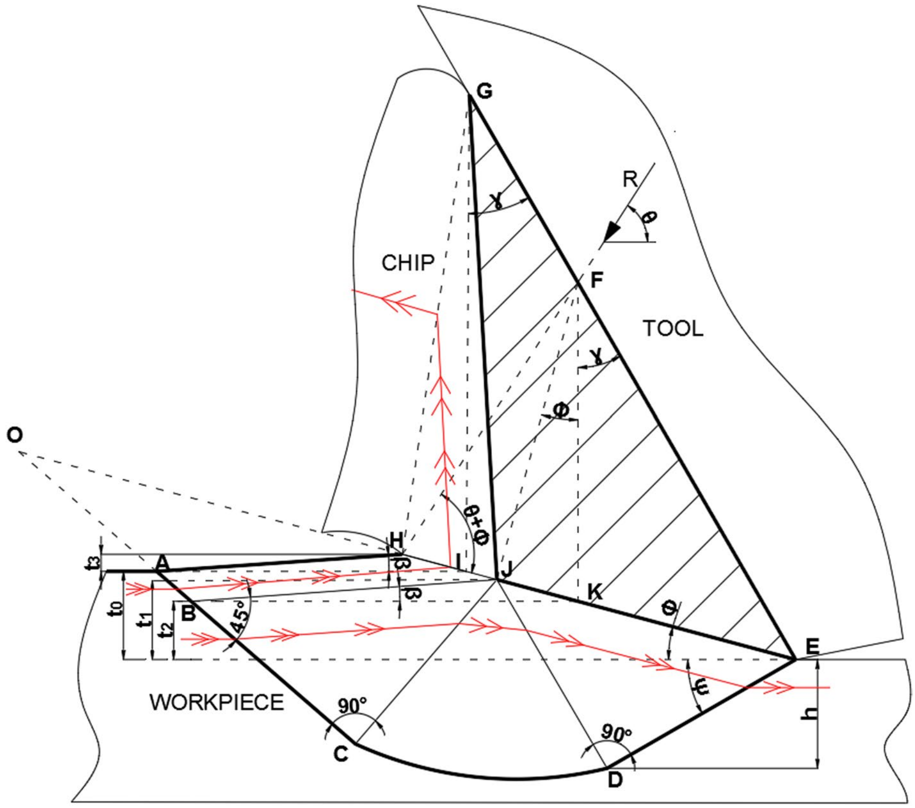

Fig. 1 Proposed slip-line field model with the cutting tool having negative rake angle

$$\Psi = \frac{\pi}{4} - \phi \tag{3}$$

$$\theta = \tan^{-1} \frac{Ft}{Fc} \tag{4}$$

A force balance was considered at the lower boundary of the plastic deformation region ACDE for the new slip-line model with negative rake angle. The stresses on ACDE are shown in Fig. 2.

The forces acting on the workpiece must be in equilibrium with the forces acting on the cutting tool. Therefore, the force components affecting the workpiece can be calculated knowing the geometry of the lower boundary of the plastic deformation zone and the stress distribution on it and these forces can be taken equal to the forces on the cutting tool. This can be done without specifying the upper boundary of the deformation zone (Manjunathaiah and Endres, 2000). To achieve results, the geometry and stress distribution at the lower deformation boundary must be well estimated. At this point, it is necessary to consider the stress distribution on the ACDE. Shear stress is uniformly distributed over the ACDE. Accordingly, it is assumed that the normal stresses P_1, P_2, and P_3 act along AC, CD and DE slip lines, respectively.

Normal stresses on AC, CD and DE slip lines are expressed as:

$$P_1 = k.(1 + 2.\beta) \tag{5}$$

$$P_2 = k.\left[1 + 2\left(\frac{\pi}{4} - \frac{\phi}{2} - \frac{\beta}{2}\right)\right] \tag{6}$$

$$P_3 = k.\left[1 + 2\left(\frac{\pi}{4} - \frac{\phi}{2} - \frac{\beta}{2}\right)\right] \tag{7}$$

Cutting and thrust force equations are written as follows. Force equations are written on the basis of unit workpiece width.

$$Fc = \left\{ \begin{array}{l} \left[\tau.\cos\left(\frac{\pi}{4} - \beta\right) + P_1.\sin\left(\frac{\pi}{4} - \beta\right)\right].AC + \left[\tau.\cos\left(\frac{\phi}{2} - \frac{\beta}{2}\right) + P_2.\sin\left(\frac{\phi}{2} - \frac{\beta}{2}\right)\right].CD + \\ + \left[\tau.\cos\left(\frac{\pi}{4} - \phi\right) - -P_3.\sin\left(\frac{\pi}{4} - \phi\right)\right].DE \end{array} \right\} \Big/ 1000 \tag{8}$$

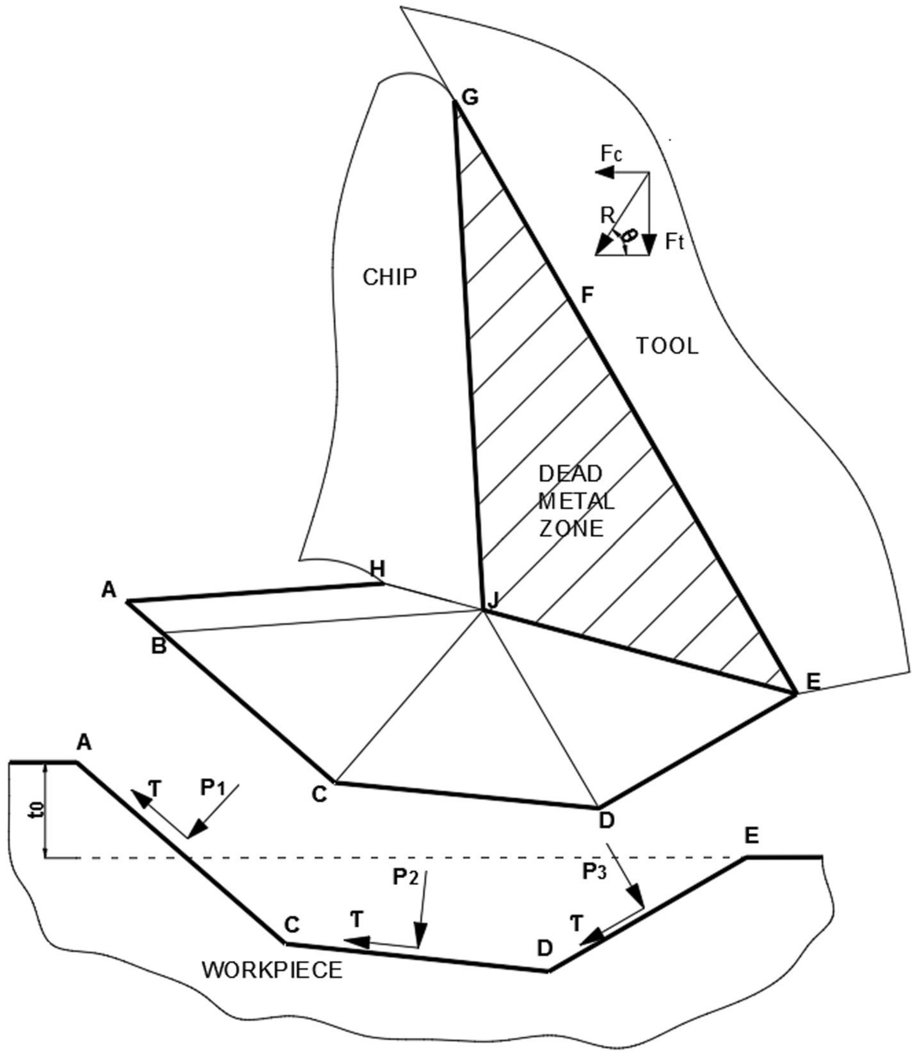

Fig. 2 Stress distribution at the lower boundary of the shear zone

$$Ft = \left\{ \begin{array}{l} \left[-\tau.\sin\left(\frac{\pi}{4}-\beta\right)+P_1.\cos\left(\frac{\pi}{4}-\beta\right)\right].AC + \left[-\tau.\sin\left(\frac{\phi}{4}-\frac{\beta}{2}\right)+P_2.\cos\left(\frac{\phi}{4}-\frac{\beta}{2}\right)\right].CD+ \\ +\left[\tau.\sin\left(\frac{\pi}{4}-\phi\right)+P_3.\cos\left(\frac{\pi}{4}-\phi\right)\right].DE \end{array} \right\} \Big/ 1000 \tag{9}$$

The AC, CD and DE slip lines are found by using geometric relations from the model. Additionally, part (t_2) of the material moving to the under of cutting tool, t_1 and h can also be determined from the model. In the calculations, the point "O" in Fig. 1 was used. AC slip line is written as follows;

$$AC = AB + BC \tag{10}$$

$$\mathrm{AB} = \frac{t_0 - t_2}{\sin\left(\frac{\pi}{4}-\beta\right)} \tag{11}$$

The angle of β and t_2 is written as follows;

$$\beta = \sin^{-1}\left(\frac{\tan\phi.\sin\phi}{\tan(\phi+\gamma)}\right) \tag{12}$$

$$t_2 = \left[\frac{(t_0+t_3).\sin(\phi+\theta)}{\cos(\gamma-\theta)}\right].[\sin(\phi+\gamma) - \tan\phi.\cos(\gamma+\phi)] \tag{13}$$

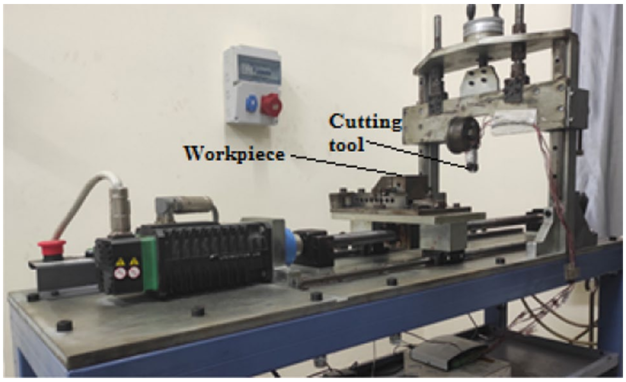

Fig. 3 Shaping-based quick stop device utilized in experimental studies

3 Experimental studies

CuZn30 (MS70) was used as workpiece material in orthogonal cutting tests. The selected material is easy for hot and cold forming and provides easy microscopic examination of slip line areas that occur during cutting process. The specimens were prepared for the experiments within the dimensions of 30 × 30 × 1.5 mm. Mechanical properties and composition of CuZn30 (Ms70) are given in Table 1.

A TPGN160308 uncoated carbide insert with no cutting edge radius was used in the experiments. The cutting insert is not exactly sharp. Natural edge radius of the cutting insert is 5 μm. In particular, the cutting edge is not rounded. The relief angle of the insert was 11°. In order to examine the plastic deformation on the workpiece, deformation at the tool–chip interface and the formations on the cutting tool tip during orthogonal cutting, a shaping-based quick stop test device was utilized. The shaping-based quick stop test device is shown in Fig. 3. The orthogonal cutting tests were performed at different depths of cut and cutting speeds. The cutting and thrust forces were measured by using strain gage and strain gage indicator on the quick stop test device. Single plane strain gages were bonded to four facets of the tool holder for force measurement. CE eDAQ V3.8.6a software program was used for collecting data, adjusting channels, and identifying strain gages. Achieved parameters were booked down in ".sif" format. The software is called InField 1.6.2, which is published by Somat Corporation and used to display the saved files. The maximum thickness and width of the chip that can be machined by the device are 2 and 1.5 mm, respectively. The quick stop device can operate at the maximum cutting speed of 17.5 m/min. There are two basic motions in the quick stop device; one of them is the cutting motion, and the other is the depth of cut motion.

$$t_3 = \frac{\left[t_0.\sin(\theta+\phi).\sin(\phi+\gamma).\sin(\phi+\beta).\sin\left(\frac{\pi}{4}-\beta\right).\tan(\phi).\cos(\gamma+\phi)\right] - \left[\left(t_0-t_2\right).\sin(\phi).\cos(\gamma-\theta).\sin\left(\frac{\pi}{4}-\beta-\phi\right).\tan(\phi).\cos(\gamma+\phi)\right]}{\left[\cos(\gamma-\theta).\sin\left(\frac{\pi}{4}-\beta\right).\sin((\phi+\beta)).\sin(\phi+\gamma)\right] - \left[in(\theta+\phi).\sin(\phi+\gamma).\sin(\phi+\beta).\sin\left(\frac{\pi}{4}-\beta\right).\tan(\phi).\cos(\gamma+\phi)\right]} \tag{14}$$

The DE slip line is written as follows;

$$BC = DE = \frac{h}{\sin\phi.\sqrt{2}} \tag{15}$$

$$h = \frac{t_1.\sin\Psi}{\sin\phi.\sqrt{2}} \tag{16}$$

$$t_1 = \frac{(t_0+t_3).\sin(\phi+\theta).\sin(\phi+\gamma)}{\cos(\gamma-\theta)} \tag{17}$$

The CD slip line is written as follows;

$$CD = \frac{t_1.\sin(\phi+\beta)}{\sin\phi.\sqrt{2}.\sin\left(\frac{\pi}{4}-\frac{\phi}{2}+\frac{\beta}{2}\right)} \tag{18}$$

Table 1 Characteristics of the workpiece material

ChemicalComposition					MechanicalProperties				
Cu(%)	Zn(%)	Pb(%)	Fe(%)	Ni(%)	Yield strength (N/mm^2)	Tensile strength (N/mm^2)	Elongation (%)	Elastic modulus (kN/mm^2)	Hardness (HV)
69,73	30,216	0,006	0,008	0,04	320	440	11	114	120

Table 2 Cutting parameters

Experiment Group No	Cutting speed (m/min)	Depth of cut(μm)	Rake angle(°)
1	0.25 – 0.5 – 0.75	50 – 100–150	– 10
2	0.25 – 0.5 – 0.75	50 – 100–150	– 30
3	0.25 – 0.5 – 0.75	50 – 100–150	– 50
4	0.25 – 0.5 – 0.75	50 – 100–50	– 70

The cutting motion at the quick stop device is provided by a servo motor and a driver. The work is performed at various rake angles. In order to secure this, a special tool holder was designed to rotate the cutting insert [37].

In the experimental studies, the amount (t_{2m}) of the depth of cut moved to the under of cutting tool was defined after each experiment. This process was carried out by measuring the weight of the workpiece sample on a precision scale before and after the orthogonal cutting. The t_{2m} values found from experimental studies were obtained by using the following equation.

$$\frac{M_1}{M_2} = \frac{a}{a - (t_0 - t_{2m})} \tag{19}$$

where a refers to the height of the work piece, M_1 is the initial weight of the work piece, M_2 is the final weight of the work piece, t_{2m}, t_2 values are found from the experiments, and t_0 is the depth of cut.

The orthogonal cutting operations were performed at four different negative rake angles, three different cutting speeds and three different depths of cut. A total of 36 experiments were conducted. Machining parameters are given in Table 2. The orthogonal quick stop test device was calibrated to measure the cutting and thrust forces. To obtain cutting and thrust forces, micro-strain values were read from the strain gages connected to the cutting tool and these values were converted into force values with calibration equations.

The workpiece was not cut through its length and the quick stop device was stopped suddenly during orthogonal cutting for the investigation of shear zone and dead metal zone. As a result, the chip was not broken and kept in contact with workpiece. The samples obtained in this way were embedded in bakelite for use in sanding, polishing and etching processes. Sanding and polishing processes were done with a grinder/polisher device. Firstly, sanding operations were carried out using 400, 800, 1000 and 1200 sandpapers, respectively. Then, polishing processes were carried out using 0.5 and 1 μm diamond paste. After sanding and polishing processes, the samples were etched for about 10 s using 100 ml of distilled water, 96 ml of ethanol and 59 g of

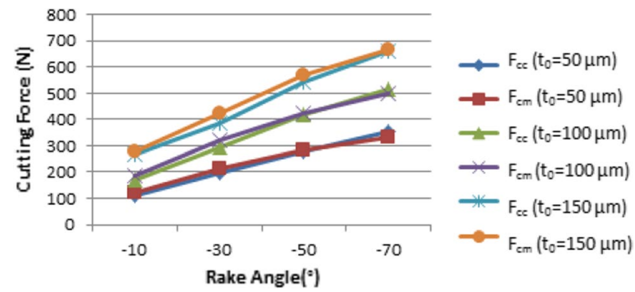

Fig. 4 Cutting forces obtained from the model (F_{cc}) and from the experiment (F_{cm}) at different depths of cut and cutting speed of 0.25 m/min

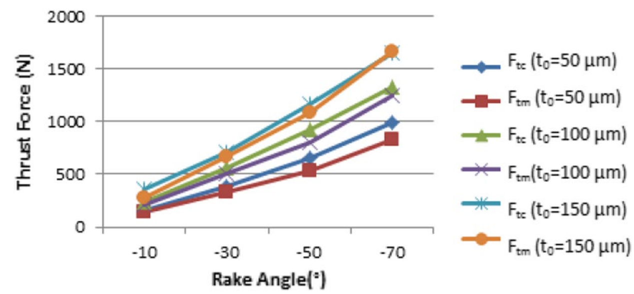

Fig. 5 Thrust forces obtained from the model (F_{tc}) and from the experiment (F_{tm}) at different depths of cut and cutting speed of 0.25 m/min

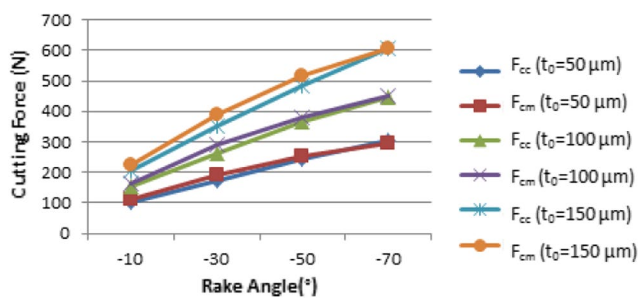

Fig. 6 Cutting forces obtained from the model (F_{cc}) and from the experiment (F_{cm}) at different depths of cut and cutting speed of 0.5 m/min

$FeCl_3$ solution. An optical microscope was used to examine the etched brass samples.

4 Results and discussion

The solutions of a slip-line field model were realized. In this regard, the experimental studies were conducted to validate the new slip-line model. According to the variations in rake angle, cutting speed and depth of cut, the cutting forces (F_c) and thrust forces (F_t) obtained from the model

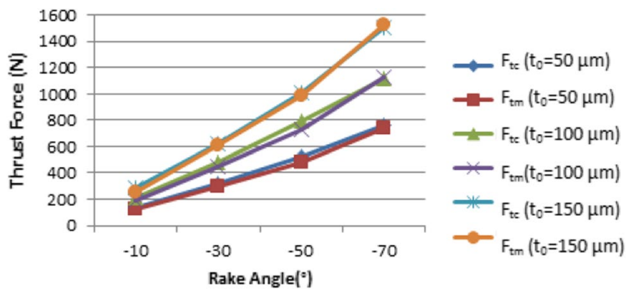

Fig. 7 Thrust forces obtained from the model (F_{tc}) and from the experiment (F_{tm}) at different depths of cut and cutting speed of 0.5 m/min

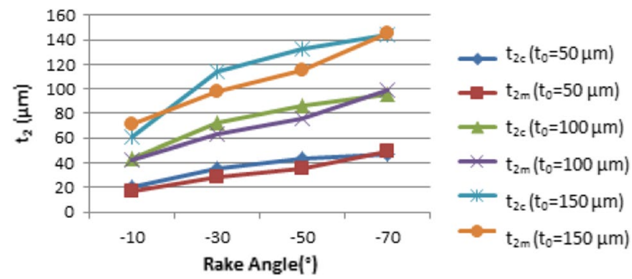

Fig. 10 The t_2 values calculated from the model (t_{2c}) and obtained from the experiments (t_{2m}) at different depths of cut and cutting speed of 0.25 m/min

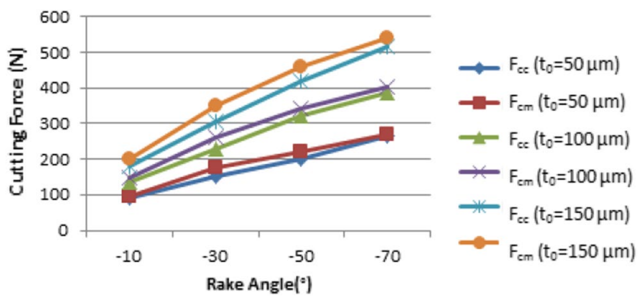

Fig. 8 Cutting forces obtained from the model (F_{cc}) and from the experiment (F_{cm}) at different depths of cut and cutting speed of 0.75 m/min

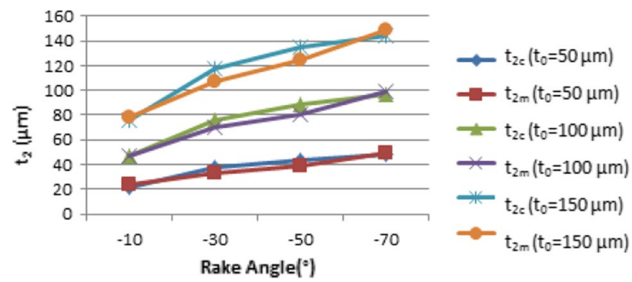

Fig. 11 The t_2 values calculated from the model (t_{2c}) and obtained from the experiments (t_{2m}) at different depths of cut and cutting speed of 0.5 m/min

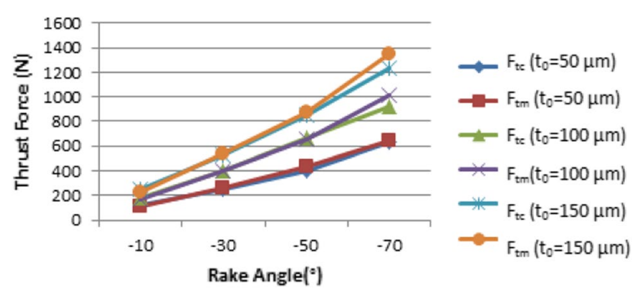

Fig. 9 Thrust forces obtained from the model (F_{tc}) and from the experiment (F_{tm}) at different depths of cut and cutting speed of 0.75 m/min

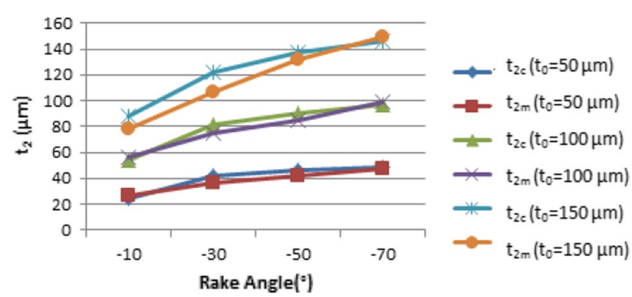

Fig. 12 The t_2 values calculated from the model (t_{2c}) and obtained from the experiments (t_{2m}) at different depths of cut and cutting speed of 0.75 m/min

and experimental studies are given in Figs. 4, 5, 6, 7, 8, 9. It can be seen that the cutting forces and thrust forces rise with increase of the negative rake angle and depth of cut. The increment of cutting speed resulted in slight decrease in cutting forces and thrust forces. The reason for reduction cutting and thrust forces with cutting speed can be explained with the increase in temperature and shortened contact length. As the depth of cut and negative rake angle increase, the plastic deformation zone becomes larger. Therefore, the cutting and thrust forces increase. High approximation was observed between the forces obtained from the experimental studies and the generated model. Experimental cutting force values were compared with the analytical cutting force values, and the model showed 6.4% average error. Experimental thrust force values were compared with the analytical thrust force values, and the model showed 5.08% average error.

Figures 10, 11, 12 show the change of the part (t_2) of the depth of cut moving to the under of the cutting tool obtained from orthogonal cutting experiments and slip-line model. The t_2 values are plotted at different negative

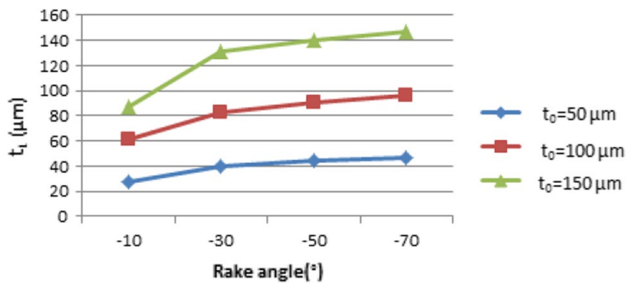

Fig. 13 The t_1 values calculated from the model with different depths of cut at cutting speed of 0.25 m/min

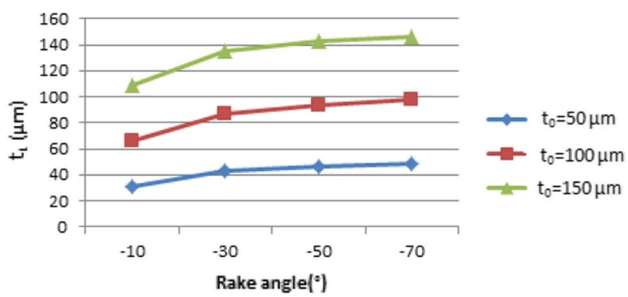

Fig. 14 The t_1 values calculated from the model with different depths of cut at cutting speed of 0.5 m/min

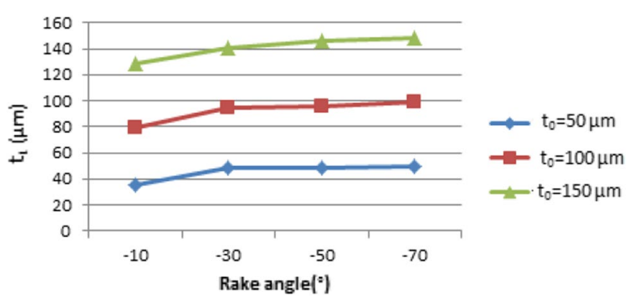

Fig. 15 The t_1 values calculated from the model with different depths of cut at cutting speed of 0.75 m/min

rake angles and cutting speeds according to different depths of cut. It can be seen that t_2 values defined experimentally and calculated from the model increased as the negative rake angle increased. In other words, as the negative rake angle increased, most of material that belong to depth of cut moved to the under of the cutting tool. As the rake angle becomes negative, the amount (t_2) of material moving to the under of the cutting tool increases. This is because the plastic deformation zone in the cutting zone becomes larger when the negative rake angle increases. As the cutting speed increases, the amount (t_2) of material going under the cutting tool also increases. When the cutting speed increases, the t_1 length decreases. This situation

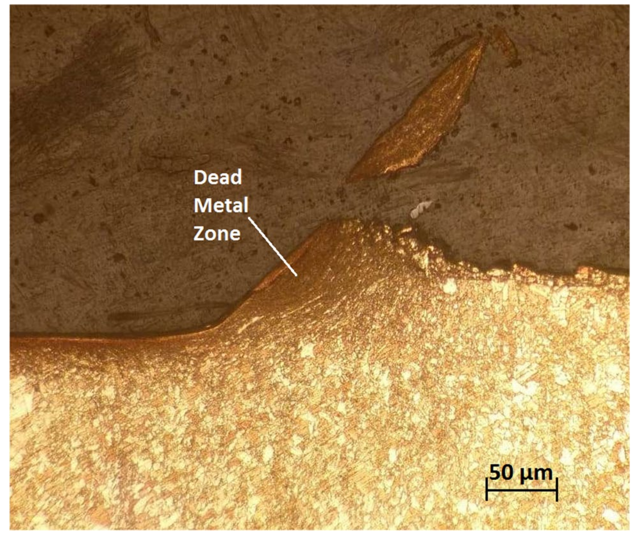

Fig. 16 Microscopic image of the cutting zone of workpiece (Cutting speed: 0.5 m/min, depth of cut: 50 µm, rake angle: − 50°)

is also stated in Ozturk's [34] study. That is, the angle ϕ in the model gets smaller, and the J point goes down. The negative rake angle impact brought on by the dead zone grows as t_1 decreases. The growth of the negative rake angle increases the amount of material moving to the under of the cutting tool. It could be seen that the results obtained from the experimental studies and the model were compatible. Experimental t_2 values were compared with the analytical t_2 values, and the model showed 4.37% average error.

Figures 13, 14, 15 show the t_1 (position of dead metal zone) values calculated from the slip-line model with different depths of cut and different cutting speeds. The t_1 value increased at all cutting speeds as the rake angle increased from − 10 to − 70°. As the rake angle becomes negative, t_1 rises. That is, the stagnation point moves up. However, it is seen that the effect of t_1 decreases as the negative rake angle increases.

In Fig. 16, as a result of microscopic examination of the cutting zone, a stagnant zone (dead metal zone) occurred in cutting with negative rake angle tool was observed. The presence of the dead metal zone accepted in the model was also seen in this figure.

5 Conclusions

In this study, a new slip-line field model for orthogonal cutting with cutting tool having negative rake angle was developed. Material flow and dead metal region were considered in this model. The generated slip-line model with negative rake angle shows that the material flow in the cutting zone is bidirectional in orthogonal cutting. In the model, a part of the depth of cut becomes chip, while the rest moved to the under of cutting tool from the separation point in front of the dead metal zone. The experimental studies were carried out by the orthogonal quick stop test device, and the cutting force and thrust force under different cutting conditions and the part of the depth of cut moved to the under of the cutting tool were determined. The results obtained are summarized as follows:

- The material flow under the cutting tool having negative rake angles was presented within a new model and experimental studies.
- In the microscopic examination of the orthogonal cutting zone, a dead metal zone in front of the cutting tool was observed.
- It was experimentally observed that the material exhibited bidirectional flow during cutting with tool having negative rake angle. The generated slip line model also enabled bidirectional material flow.
- The amount of material moving to the under of cutting tool changed depending on the cutting conditions and negative rake angle, and this amount material increased as the rake angle increased from -10 to -70°.
- The position (t_1) of the stagnation point which determines the material flow can be determined with this model.
- The amount (t_2) of the material that flowed to the under the cutting tool could be predicted by the generated model.
- The average error between experimental results and model predictions is 6,4% for cutting force, 5,08% for thrust force and 4,37% for the amount (t_2) of material moving to the under of the cutting tool. It was seen that the model and the experimental results showed high compatibility.

Acknowledgments This work was supported by Research Fund of the Yildiz Technical University [Project Number: FDK-2018-3333].

References

1. Connolly R, Rubenstein C (1968) The mechanics of continuous chip formation in orthogonal cutting. Int J Machine Tool Des Res 8(3):159–187
2. Kopalinsky EM, Oxley PLB (1984) An investigation of the influence of feed and rake angle on the ratio of feed force to cutting force when machining with negative rake angle tools. CIRP Ann 33(1):43–46
3. Abdelmoneim ME, Scrutton RF (1973) Post-machining plastic recovery and the law of abrasive wear. Wear 24(1):1–13
4. Abdelmoneim ME, Nasser AA, Abdelmahboud AM (1983) A fundamental study of cutting employing orthogonal negative rake tools. Wear 85(2):171–180
5. Findley WN, Reed RM (1963) The influence of extreme speeds and rake angles in metal cutting. J Manuf Sci Eng 85(1):49–64
6. Ding Y, Shi G, Zhang H, Han D (2020) Analysis of critical negative rake angle and friction characteristics in orthogonal cutting of AL1060 and T2. Sci Progress. https://doi.org/10.1177/0036850419878065
7. Abebe M, Appl FC (1988) Theoretical analysis of the basic mechanics of abrasive processes: Part I: General model. Wear 126(3):251–266
8. Abebe M, Appl FC (1988) Theoretical analysis of the basic mechanics of abrasive processes: Part II: model of the ploughing process. Wear 126(3):267–283
9. Sedriks AJ, Mulhearn TO (1963) Mechanics of cutting and rubbing in simulated abrasive processes. Wear 6(6):457–466
10. Lortz W (1979) A model of the cutting mechanism in grinding. Wear 53(1):115–128
11. Kita Y, Hata S, Ido M (1975) Investigation of the mechanism of metal removal-New approach to the grinding mechanism. Bullet. Japan Soc. Precision Eng 9(4):113–114
12. Kita Y, Ido M, Hata S (1978) The mechanism of metal removal by an abrasive tool. Wear 47(1):185–193
13. Kita Y, Ido M, Tuji Y (1981) The influence of the cutting speed on the mechanism of metal removal by an abrasive tool. Wear 71(1):55–63
14. Komanduri R (1971) Some aspects of machining with negative rake tools simulating grinding. Int J Machine Tool Des Res 11(3):223–233
15. Ohbuchi Y, Obikawa T (2003) Finite element modeling of chip formation in the domain of negative rake angle cutting. J Eng Mater Technol 125(3):324–332
16. Ohbuchi Y, Obikawa T (2005) Adiabatic shear in chip formation with negative rake angle. Int J Mech Sci 47(9):1377–1392
17. Doyle ED (1973) On the formation of a quick-stop chip during single grit grinding. Wear 24(2):249–253
18. Oxley PLB (1989) The mechanics of machining: an analytical approach to assessing machinability. Ellis Horwood Limited, Chichester, UK
19. Abebe M, Appl FC (1981) A slip line solution for negative rake angle cutting. Trans NAMRI/SME 19:341–348
20. Kita Y, Ido M, Kawasaki N (1982) A study of metal flow ahead of tool face with large negative rake angle. ASME J Eng Industry 104:319–325
21. Fang N (2005) Tool-chip friction in machining with a large negative rake angle tool. Wear 258(5–6):890–897
22. Lee EH, Shaffer BW (1951) The theory of plasticity applied to a problem of machining. ASME Trans J Appl Mech 18:405–413
23. Vinogradov AA (2011) On chip formation in cutting metallic materials using tools with a large negative rake. J Superhard Mater 33(4):255–260
24. Zou GP, Seethaler RJ (2011) The extension of a simple predictive model for orthogonal cutting to include flow below the cutting edge. Proc Inst Mech Eng Part B: J Eng Manuf 225(9):1568–1577
25. Yellowley I (1987) A simple predictive model of orthogonal metal cutting. Int J Mach Tools Manuf 27(3):357–365
26. Ozturk S, Altan E (2012) Slip-line metal cutting model with negative rake angle. J Braz Soc Mech Sci Eng 34(3):246–252
27. Ozturk S (2012) Slip-Line modeling of machining and determine the influence of rake angle on the cutting force. Trans Can Soc Mech Eng 36(1):23–35
28. Hu C, Zhuang K, Weng J, Zhang X, Ding H (2020) Cutting temperature prediction in negative-rake-angle machining with chamfered insert based on a modified slip line field model. Int J Mech Sci 167:105273

29. Manjunathaiah J, Endres WJ (2000) A new model and analysis of orthogonal machining with an edge-radiused tool. J Manuf Sci Eng 122(3):384–390
30. Shiva PN, Padmakumar M, Sarada BN (2019) Experimental investigation to assess the effects of trumpet hone on tool life and surface quality in milling of AISI4140 steel. FME Trans 47(3):437–441
31. Zhao X, Du Y, He L, Tao M (2019) Influence of edge preparation of coated carbide tool on milling aluminum alloy 211Z. J Braz Soc Mech Sci Eng 41(2):1–11
32. Zeilmann RP, Ost CA, Fontanive F (2018) Characterization of edge preparation processes and the impact on surface integrity after milling of AISI P20 steel. J Braz Soc Mech Sci Eng 40(9):1–7
33. Padmakumar M, Shiva Pradeep N (2020) Effect of cutting edge form factor (K-factor) on the performance of a face milling tool. CIRP J Manuf Sci Technol 31:305–313
34. Ozturk S, Altan E (2013) Position of the seperation point in machining with a rounded edge tool. Proc Inst Mech Eng Part B J Eng Manuf 227(7):965–971
35. Babu BH, Rao KV, Ben BS (2021) Modeling and optimization of dead metal zone to reduce cutting forces in micro-milling of hardened AISI D2 steel. J Braz Soc Mech Sci Eng 43(3):1–17
36. Waldorf DJ, DeVor RE, Kapoor SG (1998) A slip-line field for ploughing during orthogonal cutting. J Manuf Sci Eng 120(4):693–699
37. Ozturk S, Altan E (2012) Design of a computer aided quick-stop device for study of dead metal zone formation. J Braz Soc Mech Sci Eng 34(4):501–505